A New Analytical Method for Robust Extraction of the Small-Signal Equivalent Circuit for SiGe HBTs Operating at Cryogenic Temperatures

José-Luis Olvera-Cervantes, John D. Cressler, *Fellow, IEEE*, José-Luis Medina-Monroy, Tushar Thrivikraman, *Student Member, IEEE*, Bhaskar Banerjee, *Student Member, IEEE*, and Joy Laskar, *Fellow, IEEE*

***Abstract*—We present a new analytical direct parameter-extraction methodology for obtaining the small-signal equivalent circuit of HBTs. It is applied to cryogenically operated SiGe HBTs as a means to allow circuit design of SiGe HBT low-noise amplifiers for cooled radio astronomy applications. We split the transistor into an intrinsic transistor (IT) piece modeled as a Π-topology, and the quasi-intrinsic transistor (QIT), obtained from the IT after that the base resistance (R_b) has been removed. The relations between Z–Y-parameters of the IT and QIT are then established, allowing us to propose a new methodology for determining R_b. The present extraction method differs from previous studies in that each of the model elements are obtained from exact equations that do not require any approximations, numerical optimization, or post-processing. The validity of this new extraction methodology is demonstrated by applying it to third-generation SiGe HBTs operating at liquid-nitrogen temperature (77 K) across the frequency range of 2–22 GHz.**

***Index Terms*—Base resistance, cryogenic electronics, microwave SiGe HBTs, S-parameters, small-signal equivalent circuit.**

I. Introduction

SiGe HBT technology has emerged as a viable candidate for a wide variety of highly integrated communications systems applications, spanning the RF through millimeter-wave frequency range. SiGe HBTs possess very low broadband noise and high gain at low bias current, making them uniquely suited for low-noise amplifiers (LNAs). Due to their bandgap-engineered nature, the broadband characteristics of SiGe HBTs also improve with cooling down to cryogenic temperatures [1], making them natural candidates for cooled LNAs that are needed, for instance, in radio astronomy.

Clearly, however, having an accurate small-signal model of the SiGe HBT at such cryogenic temperatures is required for meaningful circuit design, and does not exist in commercially available design kits.

In the case of field-effect transistors (FETs) (e.g., HEMTs), small-signal broadband models have generally converged to a Π-topology implementation. For HBTs, however, two different equivalent circuits have been proposed and are used: the Π topology [2]–[9] and the T-topology [10]–[21]. For HBT small-signal modeling, several different extraction methodologies have been reported, and can be generally classified into the following three groups:

1) optimization methods;
2) partial-optimization methods;
3) analytical methods.

The analytical methods can be further sub-classified into the following:

a) analytical methods requiring forward- or reverse-biased measurements or pad measurements or electromagnetic analysis, mainly to calculate the extrinsic elements;
b) direct analytical methods based on device-biased measurements and frequency approximations to determine all elements.

Optimization-based methods may be realized using commercially available computer-aided design (CAD) software, and consist of an optimization of the circuit elements until some predefined error norm is sufficiently low. Circuit elements attained by this means are lacking from a physical interpretation. Methods such as those proposed in [10], [16], [17], and [19] can be considered partial-optimization methods. In these approaches, some circuit elements are first obtained analytically from dc or RF measurements, and then the remaining model elements are determined using an optimization routine. In the direct analytical methods based on frequency approximations, such as those presented in [4], [6], and [11], mathematical expressions formulated for different ranges of operational frequency are employed. On the other hand, analytical methods based on measurements may be found in [2] and [9]. Fig. 1 depicts the conventional equivalent circuit for HBTs. Here, Z_{L1}, Z_{L2}, Z_{L3}, Y_{p1}, Y_{p2}, and Y_{p3} represent the parasitic-pad effects that are not bias dependent. The elements R_b, R_o, C_{bc}, C_π, R_π, G_{mo}, and τ represent the intrinsic transistor (IT), and

Manuscript received May 24, 2007; revised November 14, 2007. This work was supported by the National Aeronautics and Space Administration (NASA), by IBM, by the Consejo Nacional de Ciencia y TecnologÍa (CONACYT) México, by the Centro de Investigación Científica y de Educación Superior de Ensenada (CICESE), and by the Georgia Electronic Design Center, Georgia Institute of Technology.

J.-L. Olvera-Cervantes and J.-L. Medina-Monroy are with the Centro de Investigación Científica y de Educación Superior de Ensenada (CICESE), 22830 Ensenada, B.C., México (e-mail:jolvera@cicese.mx; jmedina@cicese.mx).

J. D. Cressler, T. Thrivikraman, and J. Laskar are with the School of Electrical and Computer Engineering and Georgia, Electronic Design Center, Georgia Institute of Technology Atlanta, GA 30332-0250 USA (e-mail: cressler@ece.gatech.edu; tthrivi@ece.gatech.edu; joy.laskar@ece.gatech.edu).

B. Banerjee was with the School of Electrical and Computer Engineering and Georgia, Electronic Design Center, Georgia Institute of Technology Atlanta, GA 30332-0250 USA. He is now with the Electrical Engineering Department, The Univeristy of Texas at Dallas, Richardson, TX 75080-3021 USA (e-mail: bhaskar.banerjee@utdallas.edu).

Digital Object Identifier 10.1109/TMTT.2008.916917

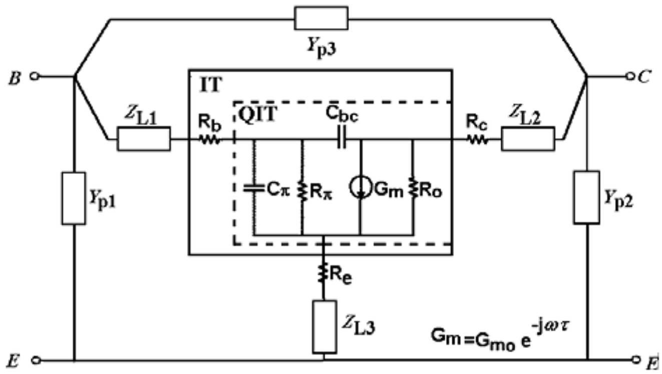

Fig. 1. Small-signal equivalent circuit for the SiGe HBT.

are bias dependent. In Fig. 1, the small-signal circuit assumes the following.

1) The base resistance R_b is composed by two parts: one extrinsic and one intrinsic. The extrinsic part is due to the pad; therefore, it is bias independent. It is implicitly considered when Z_{L1} is determined measuring a short test structure, and then removed, whereas the intrinsic R_b is determined in function of the bias point used.
2) The internal resistances R_e and R_c are determined by the linear extrapolation of the plot $\mathrm{Real}\,(Z_{12})$ and $\mathrm{Real}\,(Z_{22} - Z_{12})$ versus $1/I_b$ that gives the ordinate at the origin, whose values are R_e and R_c, respectively [16]. However, in some studies, the intrinsic R_c can be neglected in active operation [9] and with the temperature due to a conductivity enhancement [27].
3) C_{bc} is also considered to be a lumped element, and is not split into intrinsic and extrinsic contributions.

Approaches to use a distributed base–collector capacitance and base resistance (if needed) have been previously considered [22], [23]. The distributed effect on R_b can be neglected due to the low frequency range used, i.e., up to 22 GHz [27].

In this study, a new method to extract the small-signal equivalent circuit is presented. As is common practice today, we assume that the parasitic-pad effects associated with the transistor measurement structure are first removed by applying open and short structures. We establish a new procedure for obtaining the total base resistance R_b, as well as each of the other elements of the quasi-intrinsic transistor (QIT). Our method of obtaining R_b differs from previous approaches [24]–[26], and no approximations or numerical optimization or post-processing are required. This is important in the present context since R_b: 1) is important in determining the broadband noise; 2) is notoriously difficult to extract robustly; and 3) is, in principle, strongly temperature dependent and, thus, even more challenging to model at very low temperatures.

In Section II, our model extraction methodology is described, including the deembedding process needed to obtain the IT and the QIT, as well as the methodology for extracting each element of the IT. In Section III, we validate our method by applying it to small-signal model extraction of SiGe HBTs operating at 77 K across 2–22 GHz.

II. Proposed Extraction Methodology

Usually the extraction process can be divided in two stages, which are: 1) the first stage is devoted to obtaining the extrinsic elements and 2) the second stage is devoted to obtaining the intrinsic elements. Other methodologies for small-signal model extraction and deembedding of SiGe HBTs are given in [27]–[29]. As reported in [2], [16], and [30]–[33], methods to remove parasitic-pad effects in FETs and HBTs have also been proposed. Additional methods using open/short test structures were presented in [2] and [33], while others were based on forward- and reverse-bias measurements, as discussed in [16], [30], and [31]. The present method differs from these in important ways.

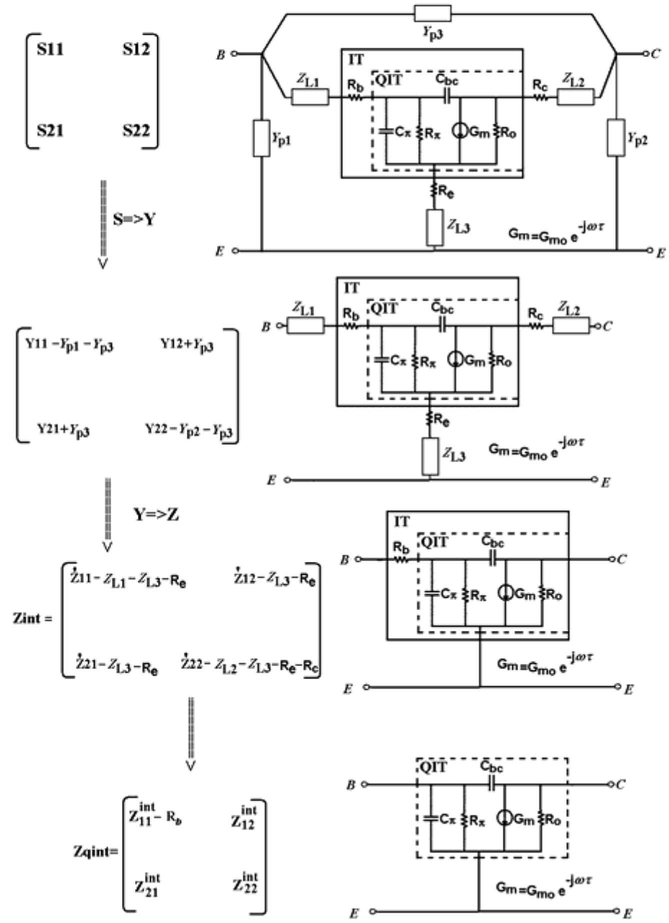

Fig. 2. Methodology for extracting the IT and QIT.

Our extraction methodology shown in Fig. 2 is based on a similar and widely used [30] Y/Z deembedding method. This procedure is used only as a tool for the deduction of the new proposed exact equations to determine the intrinsic elements of the model. Our procedure is divided into four stages.

In the first stage, S-parameters of the active transistor are measured, and then a standard deembedding process is performed to obtain the IT. In this step, admittance parasitic elements (Y_{p1}, Y_{p2}, and Y_{p3}) are determined from measurements of an open test structure, as given in [33]. Measured transistor S-parameters are transformed to Y-parameters and then Y_{p1}, Y_{p2}, and Y_{p3} are removed. The resultant matrix is transformed to Z-parameters and then R_e, R_c, Z_{L1}, Z_{L2}, and Z_{L3} are removed, where Z_{L1}, Z_{L2}, and Z_{L3} are determined from measurements of a short test structure [33].

In the second stage, intrinsic R_b is calculated, as shown on point B, beginning from the Z-parameters of the IT.

In the third stage, the QIT is obtained as shown on point C, after a deembedding process to remove R_b is performed.

In the fourth stage, each of the elements of the QIT is then calculated.

A. Theory Connecting the IT and QIT

The deembedding methodology to obtain the IT and the QIT is illustrated in Fig. 2.

The Z-parameters of the IT are then connected with the QIT using

$$Z_{11}^{\text{int}} = R_b + Z_{11}^{q\text{int}} \tag{1}$$
$$Z_{12}^{\text{int}} = Z_{12}^{q\text{int}} \tag{2}$$
$$Z_{21}^{\text{int}} = Z_{21}^{q\text{int}} \tag{3}$$
$$Z_{22}^{\text{int}} = Z_{22}^{q\text{int}} \tag{4}$$

where $Z_{ij}^{\text{int}} i,j \in \{1,2\}$ represents the Z-parameters for the IT and $Z_{ij}^{q\text{int}} i,j \in \{1,2\}$ for the QIT.

The Z-parameters for QIT are given by (5)–(8) as follows:

$$Z_{11}^{q\text{int}} = \frac{Y_{22}^{q\text{int}}}{Y_{11}^{q\text{int}}Y_{22}^{q\text{int}} - Y_{12}^{q\text{int}}Y_{21}^{q\text{int}}} \tag{5}$$
$$Z_{12}^{q\text{int}} = \frac{Y_{12}^{q\text{int}}}{Y_{11}^{q\text{int}}Y_{22}^{q\text{int}} - Y_{12}^{q\text{int}}Y_{21}^{q\text{int}}} \tag{6}$$
$$Z_{21}^{q\text{int}} = \frac{Y_{21}^{q\text{int}}}{Y_{11}^{q\text{int}}Y_{22}^{q\text{int}} - Y_{12}^{q\text{int}}Y_{21}^{q\text{int}}} \tag{7}$$
$$Z_{22}^{q\text{int}} = \frac{Y_{11}^{q\text{int}}}{Y_{11}^{q\text{int}}Y_{22}^{q\text{int}} - Y_{12}^{q\text{int}}Y_{21}^{q\text{int}}} \tag{8}$$

where

$$Y_{11}^{q\text{int}} = Y_a + Y_c \tag{9}$$
$$Y_{12}^{q\text{int}} = -Y_a \tag{10}$$
$$Y_{21}^{q\text{int}} = Y_a + G_{m0}e^{-j\omega T} \tag{11}$$
$$Y_{22}^{q\text{int}} = Y_a + Y_b \tag{12}$$
$$Y_a = j\omega C_{bc} \tag{13}$$
$$Y_b = g_0 = \frac{1}{R_0} \tag{14}$$
$$Y_c = \frac{1}{R_\pi} + j\omega C_\pi. \tag{15}$$

B. Extracting R_b

From (1), (5), and (6), we have

$$Z_{11}^{\text{int}} = R_b + \frac{Y_{22}^{q\text{int}}}{-Y_{12}^{q\text{int}}} Z_{12}^{q\text{int}}. \tag{16}$$

Substituting (10) and (12) into (16), the difference between Z_{11}^{int} and $Z_{12}^{q\text{int}}$ can then be expressed as follows:

$$Z_{11}^{\text{int}} - Z_{12}^{q\text{int}} = R_b + \frac{Y_b}{Y_a} Z_{12}^{q\text{int}}. \tag{17}$$

Now, using (13) and (14), we find

$$Z_{11}^{\text{int}} - Z_{12}^{q\text{int}} = R_b + \frac{g_0}{\omega C_{bc}} \text{Im}\left\{Z_{12}^{q\text{int}}\right\} - j\frac{g_0}{\omega C_{bc}} \text{Re}\left\{Z_{12}^{q\text{int}}\right\}. \tag{18}$$

Since the IT and QIT are connected through $Z_{12}^{\text{int}} = Z_{12}^{q\text{int}}$, the real and imaginary parts of the difference between Z_{11}^{int} and Z_{12}^{int} are given by (19) and (20) as follows:

$$\text{Re}\left\{Z_{11}^{\text{int}} - Z_{12}^{\text{int}}\right\} = R_b + \frac{g_0}{\omega C_{bc}} \text{Im}\left\{Z_{12}^{\text{int}}\right\} \tag{19}$$
$$\text{Im}\left\{Z_{11}^{\text{int}} - Z_{12}^{\text{int}}\right\} = -\frac{g_0}{\omega C_{bc}} \text{Re}\left\{Z_{12}^{\text{int}}\right\}. \tag{20}$$

Finally, the base resistance can be obtained by substituting (20) into (19) to obtain

$$R_b = \text{Re}\left\{Z_{11}^{\text{int}} - Z_{12}^{\text{int}}\right\} + \frac{\text{Im}\left\{Z_{11}^{\text{int}} - Z_{12}^{\text{int}}\right\} \text{Im}\left\{Z_{12}^{\text{int}}\right\}}{\text{Re}\left\{Z_{12}^{\text{int}}\right\}}. \tag{21}$$

Equation (21) shows that R_b can be calculated directly from the measured Z-parameters without any approximations or numerical optimizations or post-processing.

C. Extracting the Elements of the QIT

Following the deembedding procedure shown in the Fig. 2, the Y-parameters of the QIT can now be obtained. Using (9) and (10), the elements of the QIT can be written as

$$C_{bc} = \frac{\text{Im}\left\{-Y_{12}^{q\text{int}}\right\}}{\omega} \tag{22}$$
$$g_0 = \text{Re}\left\{Y_{12}^{q\text{int}} + Y_{22}^{q\text{int}}\right\} \tag{23}$$
$$\frac{1}{R_\pi} = \text{Re}\left\{Y_{11}^{q\text{int}} + Y_{12}^{q\text{int}}\right\} \tag{24}$$
$$C_\pi = \frac{\text{Im}\left\{Y_{11}^{q\text{int}} + Y_{12}^{q\text{int}}\right\}}{\omega} \tag{25}$$
$$G_{m0} = \left|Y_{21}^{q\text{int}} - Y_{12}^{q\text{int}}\right| \tag{26}$$
$$\tau = \frac{-1}{\omega} \text{Tan}^{-1}\left(\frac{\text{Im}\left\{Y_{21}^{q\text{int}} - Y_{12}^{q\text{int}}\right\}}{\text{Re}\left\{Y_{21}^{q\text{int}} - Y_{12}^{q\text{int}}\right\}}\right) \tag{27}$$

where $Y_{ij}^{\text{int}} i,j \in \{1,2\}$ are the Y-parameters of the QIT. All elements are now determined exactly using these equations without any approximations or optimization.

III. Experimental Results

In order to validate the proposed extraction technique, we have applied it to a third-generation 200-GHz (at 300 K) $0.12 \times 10\ \mu\text{m}^2$ SiGe HBT [1]. The S-parameter measurements were made in a cryogenic microwave probing system using a vector network analyzer over a frequency range of 2–22 GHz (measurement details are given in [1]). We show data up to 22 GHz, but the device has a calculated f_T more than 244 GHz.

Table I gives the extracted elements for the SiGe HBT operating at liquid–nitrogen temperature (77 K) for the following

TABLE I
EXTRACTED SMALL-SIGNAL MODEL PARAMETERS OF THE SiGe HBT AT 77 K

Element	I_B=0.001mA V_{CE}=1.200 V I_C=3.586mA	I_B=0.002mA V_{CE}=1.200 V I_C=6.004mA	I_B=0.003mA V_{CE}=1.200 V I_C=12.296mA
$R_b(\Omega)$	17.7247	17.1791	17.4730
$R_e(\Omega)$	2.921	2.921	2.921
$R_c(\Omega)$	0.1231	0.1231	0.1231
C_{bc}(fF)	12.6816	12.6596	12.6277
$C\pi$ (fF)	175.7211	249.5929	536.2895
$R_o(k\Omega)$	1.6622	1.2937	0.6546
R_π $(k\Omega)$	2.0577	1.1972	0.3749
G_{mo}(S)	0.2897	0.4683	1.1060
τ(ps)	0.7483	0.7465	0.3352

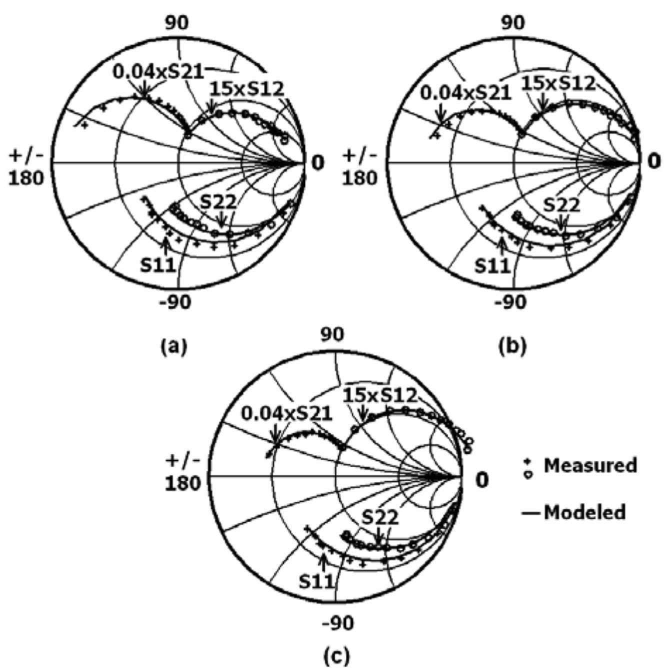

Fig. 3. S-parameters of the 0.12×10 μm^2 SiGe HBT at 77 K. (a) $Vce = 1.200$ V, $Ib = 0.003$ mA, and $Ic = 12.296$ mA. (b) $Vce = 1.200$ V, $Ib = 0.002$ mA, and $Ic = 6.004$ mA. (c) $Vce = 1.200$ V, $Ib = 0.001$ mA, and $Ic = 3.856$ mA.

three representative bias points.

1) $Vce = 1.200$ V, $Ib = 0.003$ mA, and $Ic = 12.296$ mA.
2) $Vce = 1.200$ V, $Ib = 0.002$ mA, and $Ic = 6.004$ mA.
3) $Vce = 1.200$ V, $Ib = 0.001$ mA, and $Ic = 3.856$ mA.

Fig. 3 compares the directly measured versus modeled S-parameters for the three bias points at 77 K, from 2 to 22 GHz, and shows excellent agreement between model and data. The modeled S-parameters are presented without any optimization or tuning adjustment. The worst case error in Fig. 3(a) for the phase was 8° for S_{22} for frequencies higher than 20 GHz; however, at lower frequencies, the maximum difference in phase was only 3°.

The worst case magnitude for the relative error was 4% for S_{21}. Similar errors were obtained for the other cases. Figs. 4–10 show the extracted model parameters for bias point 2) at 77 K. The statistical median was used to assign a value to each model element. This modeling methodology requires no assumptions,

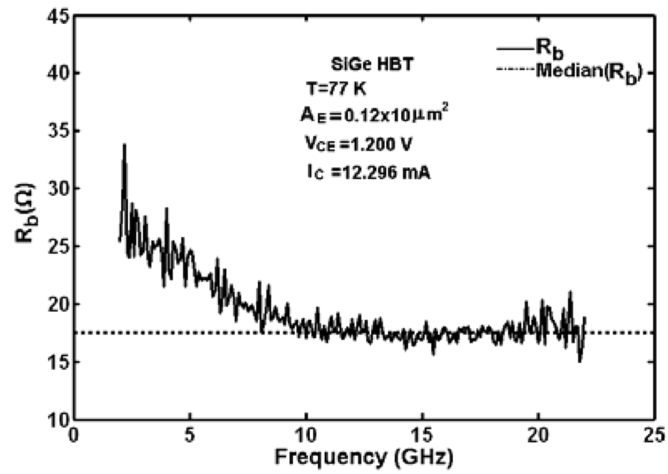

Fig. 4. Extracted base resistance as a function of frequency.

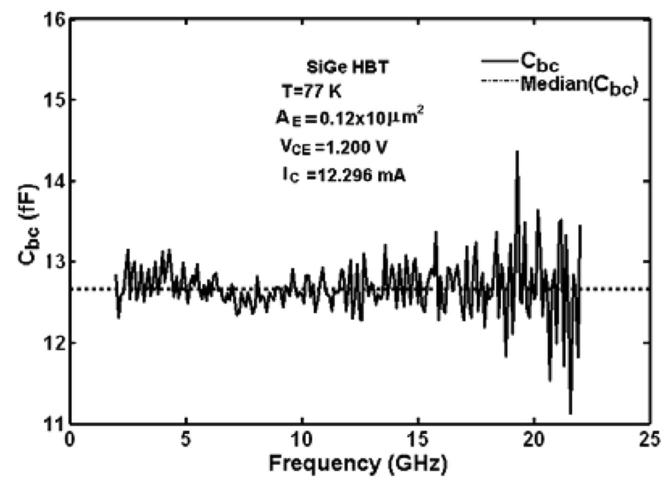

Fig. 5. Extracted base–collector capacitance as a function of frequency.

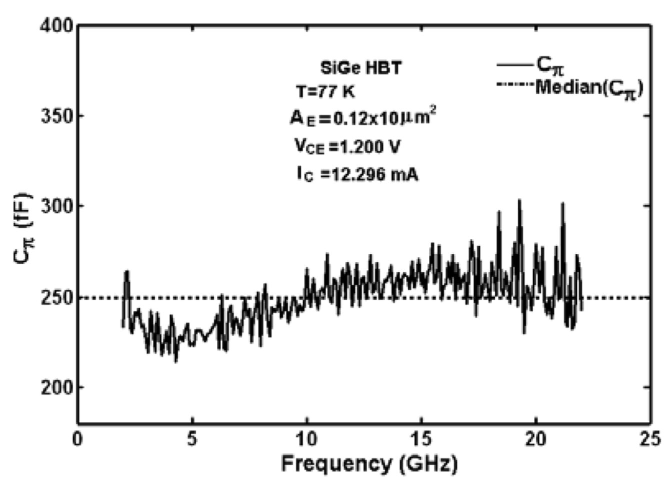

Fig. 6. Extracted base–emitter capacitance as a function of frequency.

and can be applied to any temperature at which S-parameters can be validly measured. The resultant small-signal circuit can then be used to design the requisite circuit. We note that this assumption-free modeling methodology should be extendable

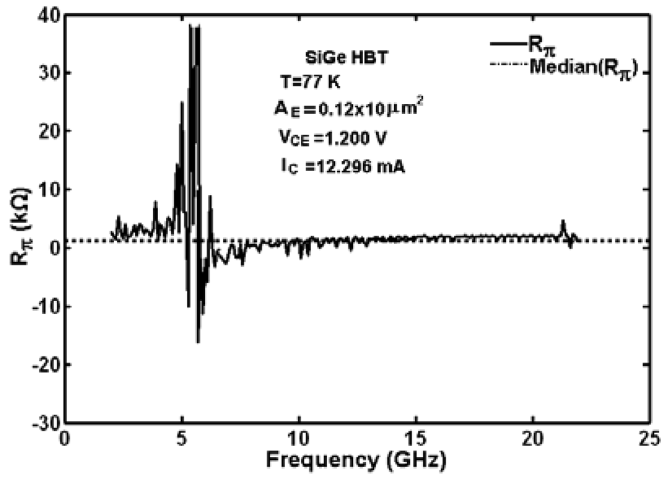

Fig. 7. Extracted base–emitter resistance as a function of frequency.

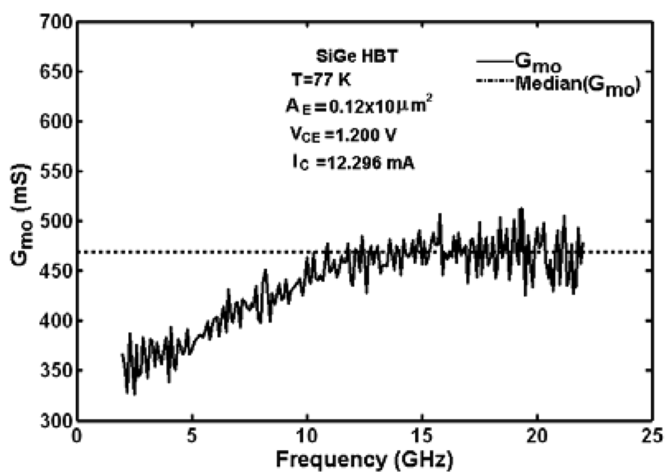

Fig. 8. Extracted transconductance as a function of frequency at 77 K.

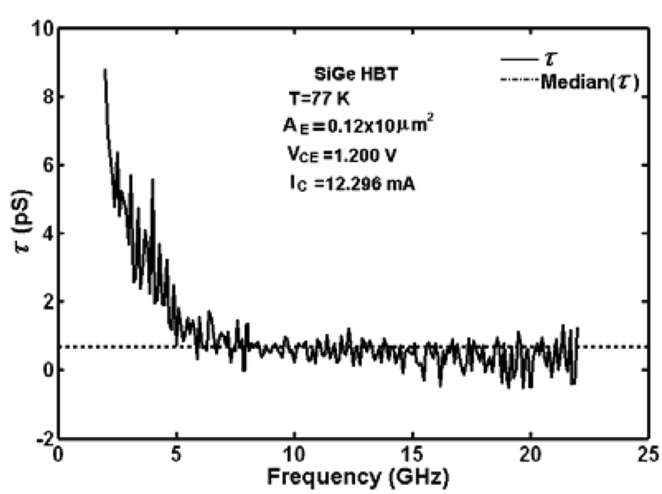

Fig. 9. Extracted collector-to-emitter delay time as a function of frequency at 77 K.

to broadband noise modeling of these devices as well, and will be reported at a later date.

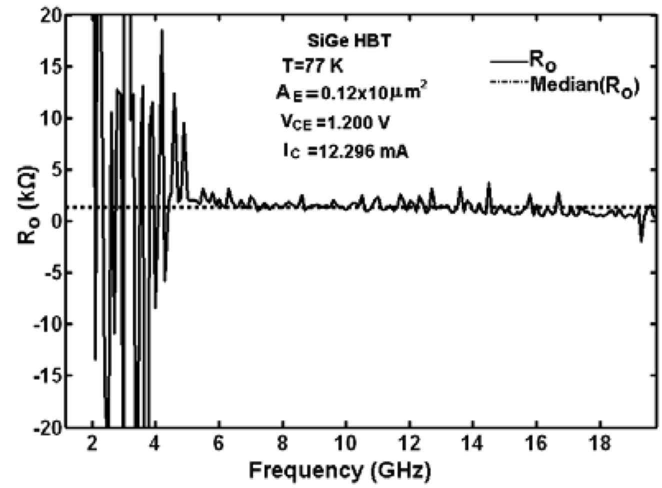

Fig. 10. Output resistance as a function of frequency at 77 K.

IV. Conclusion

A new analytical direct parameter-extraction methodology for obtaining the small-signal equivalent circuit of SiGe HBTs at cryogenic temperatures is proposed. We have established a set of closed-form equations to determine each one of the model elements. Our method differs from previous studies in that the elements (and particularly the base resistance) are obtained from exact equations and, thus, do not require any approximations or numerical optimization. The proposed method has been successfully applied to SiGe HBTs operating at 77 K, and the validity verified by direct comparison with measured data from 2 to 22 GHz.

References

[1] B. Banerjee, S. Venkataraman, Y. Lu, Q. Liang, C.-H. Lee, S. Nuttinck, D. Heo, Y.-J. E. Chen, J. D. Cressler, J. Laskar, G. Freeman, and D. C. Ahlgren, "Cryogenic operation of third-generation, 200 GHz peak f_T, silicon–germanium heterojunction bipolar transistors," *IEEE Trans. Electron Devices*, vol. 52, no. 4, pp. 585–593, Apr. 2005.

[2] D. Costa, W. U. Liu, and J. S. Harris, "Direct extraction of the AlGaAs heterojunction bipolar transistor small-signal equivalent circuit," *IEEE Trans. Electron Devices*, vol. 38, no. 9, pp. 2018–2024, Sep. 1991.

[3] D. R. Pehlke, A. Sailer, W.-J. Ho, J. A. Higgis, and M. F. Chang, "Direct parametric extraction of l/f noise source magnitude and physical location from baseband spectra in HBTs," in *IEEE MTT-S Int. Microw. Symp. Dig.*, 1996, pp. 1305–1308.

[4] S. Lee, "Direct extraction of base–collector model parameters for AIGaAs/GaAs HBT equivalent circuit," *Electron. Lett.*, vol. 33, pp. 815–817, Apr. 1997.

[5] S. Lee, "Effects of pad and interconnection parasitics on forward transit time in HBT's," *IEEE Trans. Electron Devices*, vol. 46, no. 2, pp. 275–280, Feb. 1999.

[6] A. Ouslimani, J. Gaubert, H. Hafdallah, A. Birafane, P. Pouvil, and H. Leier, "Direct extraction of linear HBT-model parameters using nine analytical expression blocks," *IEEE Trans. Microw. Theory Tech.*, vol. 50, no. 1, pp. 218–221, Jan. 2002.

[7] M. Rudolph, F. Lenk, R. Doemer, and P. Heymann, "Towards a unified method to implement transit-time effects in pi-topology HBT compact models," in *IEEE MTT-S Int. Microw. Symp. Dig.*, 2002, pp. 997–1000.

[8] M. W. Dvorak and C. R. Bolognesi, "On the accuracy of direct extraction of the heterojunction-bipolar-transistor equivalent-circuit model parameters C_{Π}, C_{bc} and R_e," *IEEE Trans. Microw. Theory Tech.*, vol. 51, no. 6, pp. 1640–1649, Jun. 2003.

[9] K. Lee, K. Choi, S. Kook, D. Cho, K. Park, and B. Kim, "Direct parameter extraction of SiGe HBTs for the VBIC bipolar compact model," *IEEE Trans. Electron Devices*, vol. 52, no. 3, pp. 375–384, Mar. 2005.

[10] S. Lee and A. Gopinath, "New circuit model for RF probe pads and interconnections for extraction of HBT equivalent circuits," *IEEE Electron Device Lett.*, vol. 12, no. 10, pp. 521–523, Oct. 1991.

[11] D. R. Pehlke and D. Pavlidis, "Direct calculation of the HBT equivalent circuit from measured S-parameters," in *IEEE MTT-S Int. Microw. Symp. Dig.*, 1992, pp. 735–738.

[12] D. R. Pahlke and D. Pavlidis, "Evaluation of the factors determining HBT high-frequency performance by direct analysis of S-parameter data," *IEEE Trans. Microw. Theory Tech.*, vol. 40, no. 12, pp. 2367–2373, Dec. 1992.

[13] S. Lee and A. Gopinath, "Parameter extraction technique for HBT equivalent circuit using cutoff mode measurement," *IEEE Trans. Microw. Theory Tech.*, vol. 40, no. 3, pp. 574–577, Mar. 1992.

[14] S. A. Maas and D. Tait, "Parameter-extraction for heterojunction bipolar transistors," *IEEE Trans. Microw. Guided Wave Lett.*, vol. 2, no. 12, pp. 502–504, Dec. 1992.

[15] U. Schaper and B. Holzapfl, "Analytical parameter extraction of the HBT equivalent circuit with T-like topology from measured S-parameters," *IEEE Trans. Microw. Theory Tech.*, vol. 43, no. 3, pp. 493–498, Mar. 1995.

[16] Y. Gobert, P. J. Tasker, and K. H. Bachem, "A physical, yet simple, small-signal equivalent circuit for the heterojunction bipolar transistor," *IEEE Trans. Microw. Theory Tech.*, vol. 45, no. 1, pp. 149–153, Jan. 1997.

[17] A. Samelis and D. Pavlidis, "DC to high-frequency HBT model parameter evaluation using impedance block conditioned optimization," *IEEE Trans. Microw. Theory Tech.*, vol. 45, no. 6, pp. 886–897, Jun. 1997.

[18] Q. Cai, J. Gerber, U. L. Rodhe, and T. Daniel, "HBT high-frequency modeling and integrated parameter extraction," *IEEE Trans. Microw. Theory Tech.*, vol. 45, no. 12, pp. 2493–2502, Dec. 1997.

[19] B. Li, S. Prasad, L. Yang, and S. C. Wang, "A semi-analytical parameter-extraction procedure for HBT equivalent circuit," *IEEE Trans. Microw. Theory Tech.*, vol. 46, no. 10, pp. 1427–1435, Oct. 1998.

[20] M. Rudolph, R. Doerner, and P. Heymann, "Direct Extraction of HBT Equivalent-Circuit Elements," *IEEE Trans. Microw. Theory Tech.*, vol. 47, no. 1, pp. 82–84, Jan. 1999.

[21] B. Li and S. Prasad, "Basic expressions and approximations in small-signal parameter extraction for HBT's," *IEEE Trans. Microw. Theory Tech.*, vol. 47, no. 5, pp. 534–539, May 1999.

[22] A. Raghavan, S. Venkataraman, B. Banerjee, Y. Suh, D. Heo, and J. Laskar, "Direct extraction of an empirical temperature-dependent InGaP/GaAs HBT large-signal model," *IEEE J. Solid-State Circuits*, vol. 38, no. 9, pp. 1443–1450, Sep. 2003.

[23] Y. Suh, D. Heo, A. Raghavan, E. Gebara, S. Nuttinck, K. Lim, and J. Laskar, "Direct extraction and modeling method for temperature dependent large signal CAD model of Si-BJT," in *IEEE MTT-S Int. Microw. Symp. Dig.*, 2001, pp. 971–974.

[24] J. D. Cressler and G. Niu, *Silicon–Germanium Heterojunction Bipolar Transistors*. Norwood, MA: Artech House, 2003, pp. 149–151.

[25] T. Nakadai and K. Hashimoto, "Measuring the base resistance of bipolar transistors," in *Proc. IEEE Bipolar Circuits Technol. Meeting*, 1991, pp. 200–203.

[26] W. Kloosterman, J. Paasschens, and D. Klaassen, "Improved extraction of base and emitter resistance from small signal high frequency admittance measurements," in *Proc. IEEE Bipolar Circuits Technol. Meeting*, 1999, pp. 93–96.

[27] S. Pruvost, S. Delcourt, I. Telliez, M. Laurens, N.-E. Bourzgui, F. Danneville, A. Monroy, and G. Dambrine, "Microwave and noise performance of SiGe BiCMOS HBT under cryogenic temperatures," *IEEE Electron Device Lett.*, vol. 26, no. 12, pp. 105–108, Dec. 2005.

[28] S. Delcourt, G. Dambrine, N. E. Bourzgui, S. Lepilliet, C. Laporte, J. P. Fraysse, and M. Maignan, "A non-uniform thermal de-embedding approach for cryogenic on-wafer high frequency noise measurements," in *IEEE MTT-S Int. Microw. Symp. Dig.*, 2004, pp. 1809–1812.

[29] B. Sheinman, E. Wasige, M. Rudolph, R. Doerner, V. Sidorov, S. Cohen, and D. Ritter, "A peeling algorithm for extraction of the HBT small signal equivalent circuit," *IEEE Trans. Microw. Theory Tech.*, vol. 50, no. 12, pp. 2804–2810, Dec. 2002.

[30] G. Dambrine, A. Cappy, F. Heliodore, and E. Playez, "A new method for determining the FET small-signal equivalent circuit," *IEEE Trans. Microw. Theory Tech.*, vol. 36, no. 7, pp. 1151–1159, Jul. 1988.

[31] A. Miras and E. Legros, "Very high-frequency small-signal equivalent circuit for short gate-length InP HEMTs," *IEEE Trans. Microw. Theory Tech.*, vol. 45, no. 7, pp. 1018–1026, Jul. 1997.

[32] R. Tayrani, J. E. Gerber, T. Daniel, R. S. Pengelly, and U. L. Rohde, "A new and reliable direct parasitic extraction method for MESFETs and HEMTs," in *Proc. 23rd Eur. Microw. Conf.*, Sep. 1993, pp. 451–453.

[33] M. C. A. M. Koolen, J. A. M. Geelen, and M. P. J. G. Versleijen, "An improved de-embedding technique for on-wafer high-frequency characterization," in *Proc. IEEE Bipolar Circuits Technol. Meeting*, 1991, pp. 188–191.

José-Luis Olvera-Cervantes received the B.S. degree in physics and mathematics from the Instituto Politécnico Nacional (IPN). México City, México, in 2001, the M.S. degree in electronic and telecommunications from the Centro de Investigación Científica y de Educación Superior de Ensenada (CICESE), Ensenada, B.C. Mexico, in 2005, and is currently working toward the Ph.D. degree in high-frequency electronics at CICESE.

His research interests are in the field of modeling and characterization of small-signal equivalent-circuit parameter-extraction techniques for HBT, MOSFET, and HEMT models for use in the design of high-frequency integrated circuits at room and cryogenic temperatures.

John D. Cressler (S'86–A'91–SM'91–F'01) received the Ph.D. degree in applied physics from Columbia University, New York, NY, in 1990.

From 1984 to 1992, he was on the research staff with IBM Research. From 1992 to 2002, he was a member of the faculty with Auburn University. He is currently Ken Byers Professor of Electrical and Computer Engineering with the Georgia Institute of Technology, Atlanta. He has authored or coauthored over 350 papers. He coauthored *Silicon–Germanium Heterojunction Bipolar Transistors* (Artech House, 2003). He edited *Silicon Heterostructure Handbook: Materials, Fabrication, Devices, Circuits, and Applications of SiGe and Si Strained-Layer Epitaxy* (CRC, 2006). His research interests concern silicon-based heterostructure devices and circuits.

Dr. Cressler has served as an associate editor for three IEEE journals. He has been a member of numerous conference program committees. He has been the recipient of numerous awards for both his teaching and research.

José-Luis Medina-Monroy received the B.S.E.E. degree from the Universidad de Guadalajara, Guadalajara, México, in 1978, and received the M.Sc. and Ph.D. degrees from the Centro de Investigación Científica y de educación Superior de Ensenada (CICESE), Ensenada, B.C., México, in 1982 and 1994, respectively.

Since 1982, he has been a Professor and Researcher of the High-Frequency Group, CICESE. His research has focused on characterization of microwave transistors, linear and nonlinear analysis, design of LNAs, DROs, filters, electromagnetic analysis of planar circuits (microstrip and coplanar waveguide), on-wafer characterization of pseudomorphic HEMTs (pHEMTs) and modeling of S-parameters and noise parameters at cryogenic temperatures, design of cryogenic amplifiers, analysis and design of microwave antennas (reflector and patch-antenna arrays), as well as the design of RF communications systems up to 40 GHz for satellite and radio-astronomy applications.

Tushar Thrivikraman (S'02) received the B.S. degree in electrical engineering from the Georgia Institute of Technology, Atlanta, in 2002, the B.B.A. degree in decision and information analysis from the Goizueta Business School, Emory University, Atlanta, GA, in 2001. and is currently working toward the M.S. degree at the Georgia Institute of Technology.

He is currently a member of the Silicon Germanium Devices and Circuit Research Team, Georgia Institute of Technology. Prior to joining the Georgia Institute of Technology, he was with the Combat Sustainment Wing, Warner Robins Air Logistics Center, Robins Air Force Base (Robins AFB), as a Defense Career Intern, where he supported testing and sustainment operations for an electronic countermeasures radar system.

Bhaskar Banerjee (S'01) received the B.Tech. degree (Honors) in electronics and electrical communication engineering from the Indian Institute of Technology, Kharagpur, India, in 2001, and the M.S. and Ph.D. degrees in electrical and computer engineering from the Georgia Institute of Technology, Atlanta, in 2003 and 2006, respectively.

He is currently an Assistant Professor with the Electrical Engineering Department, The University of Texas at Dallas, Richardson. He was a Graduate Intern with the IBM Thomas J. Watson Research Center, Yorktown Heights, NY, and with the National Semiconductor Corporation. He was a Graduate Co-Op with RF Solutions (now a part of Anadigics Inc.) and Under-Graduate Intern with the Asia Development Center, Texas Instruments Incorporated, Bangalore, India. His research interests include modeling, analysis, and characterization of SiGe HBTs and complementary SiGe HBTs and the study of their impact on high-speed high-performance analog circuits, and analog circuit design for high-speed mixed-signal and wireless applications in silicon-based processes (SiGe BiCMOS and Si CMOS).

Joy Laskar (S'84–M'85–SM'02–F'05) received the B.S. degree in computer engineering (with math/physics minors) from Clemson University, Clemson, SC, in 1985, and the M.S. and Ph.D. degrees in electrical engineering from the University of Illinois at Urbana-Champaign, in 1989 and 1991, respectively.

Prior to joining the Georgia Institute of Technology, Atlanta, in 1995, he has held faculty positions with the University of Illinois at Urbana-Champaign and the University of Hawaii. He is the Director of the Georgia Electronic Design Center, Atlanta, GA. He heads a research group with a focus on integration of high-frequency electronics with opto-electronics and integration of mixed technologies for next-generation wireless and opto-electronic systems. He has authored or coauthored over 200 papers, several book chapters (including three textbooks in development), and numerous invited talks. He has over 20 patents pending. His research has focused on high-frequency integrated circuit design and their integration.